

See discussions, stats, and author profiles for this publication at: <https://www.researchgate.net/publication/235626231>

Modeling the temperature dependent interfacial tension between organic solvents and water using dissipative particle dynamics

ARTICLE *in* THE JOURNAL OF CHEMICAL PHYSICS · MARCH 2013

Impact Factor: 2.95 · DOI: 10.1063/1.4793742

CITATIONS

9

READS

211

2 AUTHORS:



[Estela Mayoral](#)

National Institute of Nuclear Research, Mexico

17 PUBLICATIONS 103 CITATIONS

[SEE PROFILE](#)



[Armando Gama Goicochea](#)

Stanford University

64 PUBLICATIONS 202 CITATIONS

[SEE PROFILE](#)

Modeling the temperature dependent interfacial tension between organic solvents and water using dissipative particle dynamics

E. Mayoral and A. Gama Goicochea

Citation: *J. Chem. Phys.* **138**, 094703 (2013); doi: 10.1063/1.4793742

View online: <http://dx.doi.org/10.1063/1.4793742>

View Table of Contents: <http://jcp.aip.org/resource/1/JCPSA6/v138/i9>

Published by the [American Institute of Physics](#).

Additional information on J. Chem. Phys.

Journal Homepage: <http://jcp.aip.org/>

Journal Information: http://jcp.aip.org/about/about_the_journal

Top downloads: http://jcp.aip.org/features/most_downloaded

Information for Authors: <http://jcp.aip.org/authors>

ADVERTISEMENT

Instruments for advanced science

Gas Analysis



- dynamic measurement of reaction gas streams
- catalysis and thermal analysis
- molecular beam studies
- dissolved species probes
- fermentation, environmental and ecological studies

Surface Science



- UHV TPD
- SIMS
- end point detection in ion beam etch
- elemental imaging - surface mapping

Plasma Diagnostics



- plasma source characterization
- etch and deposition process
- reaction kinetic studies
- analysis of neutral and radical species

Vacuum Analysis



- partial pressure measurement and control of process gases
- reactive sputter process control
- vacuum diagnostics
- vacuum coating process monitoring

contact Hiden Analytical for further details

HIDEN
ANALYTICAL

info@hideninc.com
www.HidenAnalytical.com

CLICK to view our product catalogue



Modeling the temperature dependent interfacial tension between organic solvents and water using dissipative particle dynamics

E. Mayoral^{1,a)} and A. Gama Goicochea^{2,b)}

¹*Instituto Nacional de Investigaciones Nucleares, Carretera México-Toluca s/n, La Marquesa Ocoyoacac, Estado de México CP 52750, Mexico*

²*Departamento de Ciencias Naturales, DCNI, Universidad Autónoma Metropolitana, Unidad Cuajimalpa, Av. Pedro Antonio de los Santos 84, México, D. F. 11850, Mexico*

(Received 12 December 2012; accepted 15 February 2013; published online 6 March 2013)

The interfacial tension between organic solvents and water at different temperatures is predicted using coarse-grained, mesoscopic Dissipative Particle Dynamics (DPD) simulations. The temperature effect of the DPD repulsive interaction parameters, a_{ij} , for the different components is calculated from the dependence of the Flory-Huggins χ parameter on temperature, by means of the solubility parameters. Atomistic simulations were carried out for the calculation of the solubility parameters for different organic compounds at different temperatures in order to estimate χ and then the a_{ij} coefficients. We validate this parametrization through the study of the interfacial tension in a mixture of benzene and water, and cyclohexane and water, varying the temperature. The predictions of our simulations are found to be in good agreement with experimental data taken from the literature, and show that the use of the solubility parameter at different temperatures to obtain the repulsive DPD parameters is a good alternative to introduce the effect of temperature in these systems.

© 2013 American Institute of Physics. [<http://dx.doi.org/10.1063/1.4793742>]

I. INTRODUCTION

The interfacial tension that arises from the contact between immiscible fluids is a fundamental thermodynamic property, which determines the hydrodynamics and morphology of multiphase systems. Knowledge of interfacial tension data is important for industrial extraction, as is the case for petroleum recovery, for example. As the temperature in general varies along an extraction column or during the process, a better understanding of these systems cannot be achieved unless the temperature dependence of the interfacial tension is known. Several groups have published results on the measurement of interfacial tensions between organic solvents,¹ between water and hydrocarbons,² and between polymer blends³ varying the temperature, to name but a few. Experimental results have shown that the interfacial tension, γ , commonly decreases almost linearly when the temperature T is increased. Accurate values from $d\gamma/dT$ are difficult to obtain experimentally because this quantity is particularly small (usually less than 10^{-2} dyn/cm °C, much smaller than, the surface tension⁴). Some anomalous results have been reported⁵ where the authors found the existence of an interfacial tension maximum with temperature in alkanol-water mixes. However, a general trend has not yet emerged from those experiments.

On the theoretical side, the Guggenheim-Katayaman-van der Waals model^{4,6} for the surface tension gives $\gamma(T) = \gamma_0(1 - T/T_c)^\mu$, where γ_0 is a system-dependent constant,

T is the temperature, T_c is the critical temperature at which the interface becomes unstable, and μ is a critical exponent which has been found to be close to 11/9 for organic liquids,⁴ but this expression is by no means universal. Helfand *et al.*⁷⁻⁹ derived an expression for polymer-polymer interfacial tension γ in the limit of infinite molecular weight by performing a self-consistent mean field solution of a segmental diffusion equation across the interface. This expression involves the χ Flory Huggins (FH) parameter when a zero order approximation in compressibility is considered, and is given by: $\gamma = k_B T (\chi)^{1/2} B$, where k_B is the Boltzmann's constant, T the absolute temperature and $B = (\beta_A + \beta_B)/2 + (1/6)[(\beta_A - \beta_B)^2/(\beta_A + \beta_B)]$ with $\beta_i^2 = (1/6)\rho_{0i}b_i^2$ for species i equal A or B. b_i is the Kuhn statistical segment length and ρ_{0i} the density of pure i . This expression applies when the difference between β_A and β_B is small. Lack of enough information of χ parameters for the polymers involved limits any effort to check the theory against the experimental data available. For complex fluids of current interest it is not even clear if such a general expression is to be expected.

A relatively modern research approach is the performance of molecular dynamics and Monte Carlo computer simulations, which have the advantage of allowing the user to apply model force fields with well-controlled parameters and under appropriately chosen thermodynamic conditions.^{10,11} Most atomistically detailed simulations yield accurate predictions, but they typically are still computationally intensive if one wants to reach size and time scales comparable with those of experiments. This is one of the reasons that have led to the development of coarse-grained methods, where a procedure is chosen to lump groups of atoms or molecules into beads whose motion is then solved using standard simulation

^{a)}Electronic mail: estela.mayoral@inin.gob.mx.

^{b)}Author to whom correspondence should be addressed. Electronic mail: agama@correo.cua.uam.mx.

techniques. One of those methods that has enjoyed considerable success recently is the so called Dissipative Particle Dynamics (DPD),¹² where the coarse-graining beads represent momentum-carrying sections of a fluid, subjected to viscous and frictional forces, in addition to conservative forces. By its construction, DPD can reach mesoscopic length and time scales at a relatively inexpensive computational effort, at the cost of sacrificing microscopic detail.

Several groups have applied DPD for the prediction of the interfacial tension of various fluids, as a function of surfactant density at the interface,¹³ as a function salinity and surfactant concentration,¹⁴ for various values of model parameters,¹⁵ for different coarse-graining degrees,¹⁶ between an organic and different aqueous electrolyte solutions,¹⁷ etc. However, we are not aware of a systematic study focused on the temperature dependence of the interfacial tension of liquids. One notable exception is the work of Travis and collaborators,¹⁸ who proposed an alternative parametrization procedure for the DPD interaction parameters and applied it for the calculation of the conservative DPD interaction parameter at a few temperatures, for a particular system. The interfacial tension was not obtained and no general procedure to derive its temperature dependence was offered, though. Here we set ourselves to do precisely that. Our approach is based on the computation of the temperature dependence of the Flory-Huggins χ parameters by means of the calculation of the solubility parameters of water and organic solvents using atomistic molecular dynamics, we then use the standard DPD parametrization of the interaction parameters, and perform DPD simulations of the interfacial tension at different temperature. We compare with available experimental reports and find good agreement.

In Sec. II we describe briefly the DPD model. The procedure followed to obtain the temperature dependence of DPD interaction parameters is presented in full detail in Sec. III. Then, in Sec. IV our method is applied to the prediction of the temperature dependent interfacial tension of water/benzene and water/cyclohexane mixtures, and the results are compared with experimental data taken from the literature. Some conclusions are drawn in Sec. V.

II. MODEL AND METHODS

The structure of the DPD simulation method¹² is essentially the same as that of a standard molecular dynamics algorithm,¹⁰ in that it solves Newton's second law of motion using finite time steps to obtain the particles' positions and momenta from the total force. The difference resides in the functional form of the forces, as we shall explain below. Hence, the time evolution of positions and velocities of a DPD particle are calculated from the equations $\dot{\mathbf{r}}_i = \mathbf{v}_i$ and $\dot{\mathbf{F}}_i = \dot{\mathbf{v}}_i$, where \mathbf{v}_i is its velocity, \mathbf{r}_i is the position, and \mathbf{F}_i is its net force on particle i . We shall omit most technical details of the DPD method, since it is by now well known and there are several recent reviews on the topic, see for example, Ref. 19. For simplicity the masses of all particles are normally chosen to be the same and equal to the reduced unit of mass $m_i = 1$. The DPD model involves not only a conservative force (\mathbf{F}_{ij}^C), but also dissipative (\mathbf{F}_{ij}^D), and random (\mathbf{F}_{ij}^R)

components acting between any two particles i and j , placed a distance \mathbf{r}_{ij} apart. The total force is the sum of these three components. All forces between particles i and j vanish beyond a finite cutoff radius r_c , which represents the intrinsic length scale of the DPD model and it is usually chosen as the reduced unit of length, $r_c = 1$. The conservative force is given by a soft, linearly decaying repulsion which depends on a parameter called a_{ij} , which is the intensity of the repulsion between a pair of particles. This simple distance dependence of the force, which is a good approximation to the one obtained by spatially averaging a van der Waals-type interaction,²⁰ allows one to use relatively large integration time steps. This feature, coupled to the fact that the coarse-graining procedure can group several atoms or molecules into a single DPD particle, makes of this a mesoscopic technique. The strengths of the dissipative and random forces are related in a way that keeps the temperature internally fixed, $k_B T = \sigma^2/2\gamma$; k_B being Boltzmann's constant, as a consequence of the fulfillment of the fluctuation-dissipation theorem.²¹ The natural probability distribution function of the DPD model is that of the canonical ensemble, where N (the total particle number), volume V , and T are kept constant. The standard procedure to choose the conservative force parameter for particles of the same type, a_{ii} , is given by

$$a_{ii} = [(\kappa^{-1} N_m - 1)/2\alpha\rho]k_B T, \quad (1)$$

where N_m is the coarse-graining degree (number of water molecules grouped in a DPD particle), α is a numerical constant equal to 0.101, ρ is the DPD number density,²² κ^{-1} is the compressibility of the system and is defined by $\kappa^{-1} = 1/\rho_o k_B T \kappa_T = 1/k_B T (\partial p/\partial \rho_o)_T$, where ρ_o is the number density of molecules and $\kappa_T = (\partial p/\partial \rho_o)_T$ is the usual isothermal compressibility. When one chooses a coarse-graining degree equal to 3 water molecules in a DPD particle and uses the water compressibility at standard conditions, $\kappa^{-1} \approx 16$, and the parameter above is $a_{ii} = 78.3$. The parameter for different types of particles, a_{ij} , is calculated from its Flory-Huggins coefficient χ_{ij} using the relation:^{22,23}

$$a_{ij} = a_{ii} + 3.27\chi_{ij}. \quad (2)$$

The χ_{ij} parameter can be obtained through the solubility parameters^{24,25} for each component as we will describe in Sec. III. For the calculation of the interfacial tension we make use of the components of the pressure tensor, $P_{\alpha\alpha}$ ($\alpha = x, y, z$), which we obtain from the total conservative force, using the virial theorem,¹⁰ and it is given by

$$\gamma = L_z^* \left[\langle P_{zz} \rangle - \frac{1}{2} (\langle P_{xx} \rangle + \langle P_{yy} \rangle) \right], \quad (3)$$

where $\langle \dots \rangle$ indicates the ensemble average of the component of the pressure tensor. In our simulations, the interface between the immiscible fluids forms a plane perpendicular to the z -direction, which is why the interfacial tension has the form given by Eq. (3).

III. TEMPERATURE DEPENDENCE OF THE DPD INTERACTION PARAMETERS

To evaluate the effectiveness of our a_{ij} parametrization when the temperature is varied, we consider the interfacial tension between the components of a mixture of water and an organic solvent, at different temperatures. As we have mentioned in Sec. II, we can obtain the a_{ij} parameters via the Flory-Huggins (FH) interaction parameter between two components i and j , χ_{ij} , using Eq. (2). The χ_{ij} parameter is associated to the heat of mixing of the component (i) with the component (j).^{26,27} In the FH mean field theory this parameter is written in terms of the nearest-neighbor interaction energies ϵ_{ij} as $\chi_{12} = z(\epsilon_{11} + \epsilon_{22} - \epsilon_{12})/2k_B T$, where z is the lattice coordination number. Although the original formulation of FH mean field theory gives the interaction parameter χ_{ij} as independent of the concentration, proportional to T^{-1} and energetic in origin, comparisons with experiments show that the phenomenological χ_{ij} depends on polymer concentrations (ξ), and contains both energetic χ_H , and entropic contributions χ_S .²⁸⁻³¹ The FH interaction parameter and its temperature dependence for some systems has been experimentally obtained^{3,32} by small angle X-ray scattering analysis, obtaining the expression $\chi = \chi_S + \chi_H/T$. This functional form of the interaction parameter is consistent with the notion that χ may be written as the sum of an enthalpy and an entropic contribution. Some corrections to the FH mean field theory have been presented and a more complex dependence for the effective FH parameter with T has been obtained. Additional terms, which contain both the polymer concentration dependence as well as temperature dependence different from the standard T^{-1} form appear when next nearest-neighbor interaction energies are taken into account.^{28,29}

If we assume that the heat of mixing in this case is given by the Hildebrand-Scatchard regular solution theory,^{24,25,33} the χ_{ij} parameter at some temperature T can be obtained from the solubility parameters ($\delta(T)_i$ and $\delta(T)_j$) for the pure components in the mixture, from the relation

$$\chi(T)_{ij} = \frac{v_{ij}}{RT} (\delta_i(T) - \delta_j(T))^2. \quad (4)$$

Here v_{ij} is the partial molar volume and R is the gas constant. It is important to notice that this approximation is valid for non-polar components, but it has been used in polar systems with reasonable success.³⁴

The solubility parameter is a temperature dependent property, and is widely used to give a rough and ready approximation of solubility behavior. The solubility parameter of the solute i (δ_i) is given by the square root of its cohesive energy density and this is a measure of the strength of its molecular forces.³⁵ It is related with the enthalpy of vaporization, ΔH^{VAP} , and the molar volume, V_i^0 by

$$\delta_i = \sqrt{\frac{\Delta E_{coh}}{V_i^0}} = \sqrt{\frac{\Delta H^{VAP} - RT}{V_i^0}}. \quad (5)$$

The repulsive DPD parameter a_{ij} at different temperatures may then be obtained from Eqs. (1)–(3) as

$$a(T)_{ij} = a(T)_{ii} + 3.27 \frac{v_{ij}}{RT} (\delta_i(T) - \delta_j(T))^2. \quad (6)$$

We follow Groot and Warren's formulation²² and have taken like-like interaction parameters to be equal: $a(T)_{ii} = a(T)_{jj}$, with

$$a(T)_{ii} = [(\kappa^{-1}(T)N_m - 1)/2\alpha\rho]k_B T \quad (7)$$

following Eq. (1). An alternative method is to consider $a(T)_{ii} \neq a(T)_{jj}$ and use the Hildebrand solubility parameters for the heat of vaporization, following Travis *et al.*¹⁸ The temperature dependence of the isothermal compressibility has been explicitly indicated in Eq. (7), although for water can be obtained from experimental pressure data and for the temperature range we have studied it is found to be weak.³⁶ Equation (6) is the basis of our results.

In this work, the solubility parameters δ as a function of T for water, benzene, and cyclohexane, were calculated performing atomistic molecular dynamics simulations at different temperatures in order to obtain the cohesive energy density E_{coh} and then the δ values. To do this, periodic cells of amorphous fluid structures were constructed using the *Amorphous Cell* module of the *Materials Studio* suite.³⁷ The dimension of the simulation box was in both mixtures of 25 Å. Constant particle number (N), pressure (p), and temperature (NpT) dynamics simulations were performed first to equilibrate the density of the system. The COMPASS force field³⁸ was used to model the interatomic interactions. The *Discover Molecular Dynamics* engine³⁷ was used to evolve the systems, generating statistically independent structures. The results were then compared with experimental data, obtaining very good agreement with the reported values.³³ The results for the solubility parameter calculation for each component at different T are shown in Table I and presented in Figure 1. Clearly, for these systems, a weak linear decay dependence of the solubility parameters with temperature emerges and it is larger for water due to the fact that the cohesive energy density is larger, as a consequence of the H-bonds.

The a_{ii} parameter at different temperatures and the cross interaction parameters a_{ij} were calculated by means of the $\chi(T)$ parameters obtained from the solubility parameters for cyclohexane, benzene, and water (see Table II) using the relations given by Eqs. (4), (6) and (7). The volume of a DPD bead is $v_{DPD} = 3v_{water} = 90 \text{ Å}^3$.

In Figure 2, a linear relation between χ and $1/T$ is found, in agreement with nearest neighbors, mean field FH theory,^{26,27} and the small angle X-ray scattering

TABLE I. Solubility parameters (δ) and molecular volumes for benzene, cyclohexane, and water at different T . The data were obtained from atomistic molecular dynamics. See text for details.

T (K)	Vol		Vol		Vol	
	δ (J/cm ³)	(Å ³ /mol.)	δ (J/cm ³)	(Å ³ /mol.)	δ (J/cm ³)	(Å ³ /mol.)
	Benzene	Benzene	Cyclohexane	Cyclohexane	Water	Water
298	19.2369	145.775	16.8211	181.275	46.8461	30.860
303	18.9896	147.227	16.6470	182.000	46.6109	31.008
313	18.784	148.483	16.3469	184.540	46.0648	31.288
323	18.5978	149.711	16.1949	185.887	45.3419	31.189
333	18.1248	152.740	15.9592	188.082	44.8825	31.694
343	17.905	154.221	15.6396	191.429	44.2196	32.400

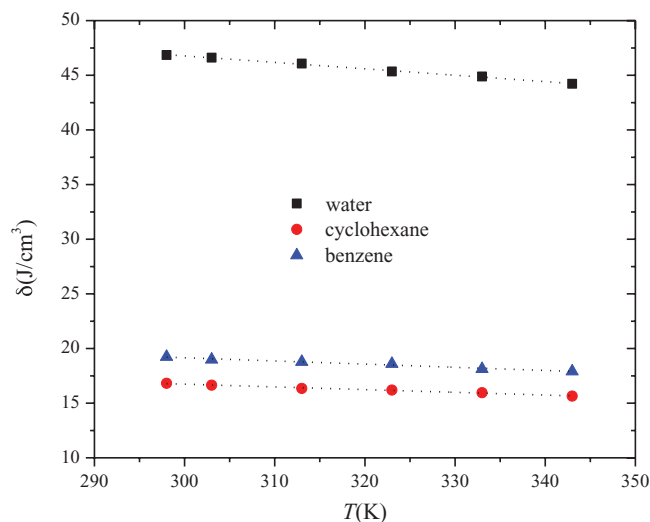


FIG. 1. Solubility parameters (δ) for cyclohexane (circles), benzene (triangles), and water (squares) at different temperature, T , obtained from atomistic molecular dynamics. The linear fits are: benzene (triangles): $\delta = -0.029 T + 27.841$; $R^2 = 0.977$; cyclohexane (circles): $\delta = -0.025 T + 24.203$; $R^2 = 0.988$. Water (squares): $\delta = -0.059 T + 64.377$; $R^2 = 0.997$.

experiments cited previously.^{3,32} Although considering next-nearest neighbors is expected to modify the linear dependence between the parameters shown in Figure 2,^{30,31} these effects should be important only when one studies systems with strong, long range Coulomb interactions. This functional dependence is expected also to be different when polymers with large molecular weight are studied, because the entropic contribution to the FH parameter becomes more important. Our methodology thus provides a route to obtain reliable values for the temperature dependence of χ , which is not easily available for many substances.

Figure 3 shows the values obtained for $a_{ij}(T)$. As we can see, the dependence of a_{ij} with temperature can be reasonably well approximated as linearly decaying. Travis *et al.*¹⁸ have found qualitatively similar temperature dependence; although their parametrization of the conservative force interaction parameters is somewhat different from ours. Notice that the interaction parameters for different types of particles shown in Figure 3 change substantially over the relatively small temperature range. In the case of monomeric mixtures the interfacial tension obtained by DPD simulations is very sensitive to this variation,¹⁵ we therefore expect an important deviation in the interfacial tension for these cases.

TABLE II. χ_{ij} and a_{ij} for water/benzene and water/cyclohexane, at different temperatures T , obtained using the relations given by Eqs. (4), (6) and (7). See text for details.

$T(K)$	$\chi_{\text{water/benzene}}$	$\chi_{\text{water/cyclohexane}}$	$a_{\text{water/benzene}}$	$a_{\text{water/cyclohexane}}$
298	5.558	6.573	96.993	100.543
303	5.471	6.438	96.690	100.072
313	5.166	6.131	95.625	98.996
323	4.812	5.715	94.383	97.542
333	4.672	5.458	93.895	96.646
343	4.387	5.174	92.900	95.652

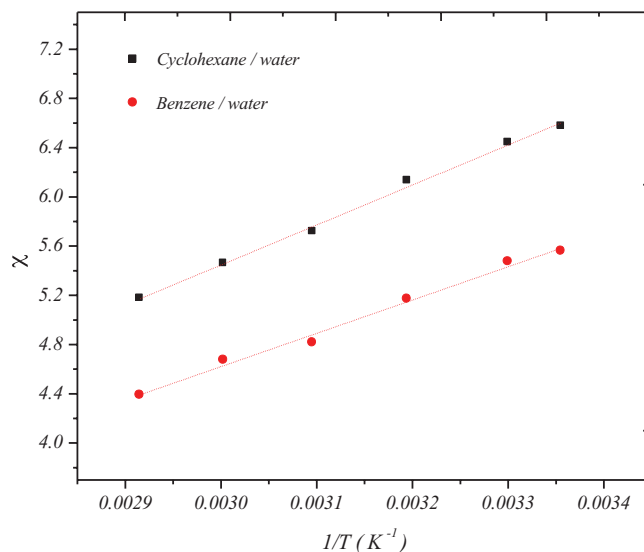


FIG. 2. Temperature dependence of the χ parameters for the water/benzene (circles), and water/cyclohexane (squares) mixtures, obtained using the relation given by Eq. (4) and the solubility parameters $\delta(T)$ presented in Table I. See text for details. The linear fits are: cyclohexane/water (black squares): $\chi = 3250.134 T^{-1} - 4.304$, with $R^2 = 0.995$; benzene/water (red circles): $\chi = 2705.72 T^{-1} - 3.497$, $R^2 = 0.990$.

IV. TEMPERATURE DEPENDENT INTERFACIAL TENSION CALCULATIONS OF BENZENE/WATER AND CYCLOHEXANE/WATER AT $T = 25^\circ\text{C}$ – 70°C

All results reported in this section were obtained from DPD simulations carried out under canonical ensemble conditions (constant density and temperature). Dimensionless units (denoted with an asterisk) were used, the dimensionless number density was obtained as $\rho^* = \rho r_c^3$ and the dimensionless repulsive parameters as $a_{ij}^* = a_{ij} r_c / k_B T$. The masses were all set equal to 1 and the total average density in the system was $\rho^* = 3.0$ in order to have a quadratic equation of

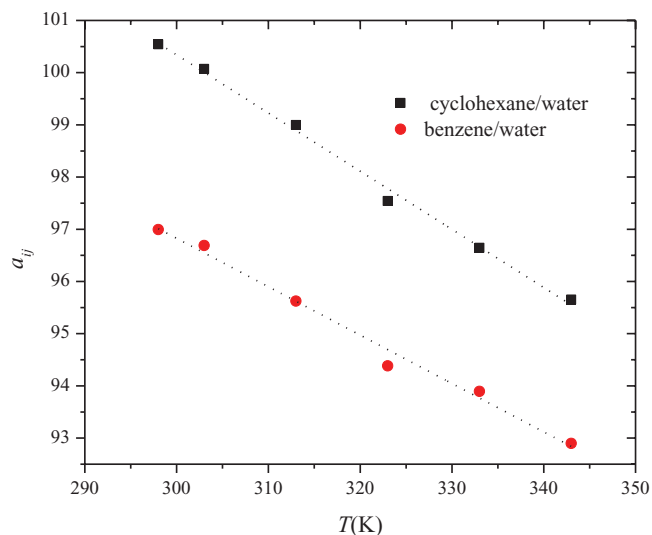


FIG. 3. Temperature dependence of a_{ij} for water/benzene (circles) and water/cyclohexane (squares) mixtures, obtained using the relations given by Eqs. (6) and (7). The linear fits (dotted lines) are: cyclohexane/water, $a_{cw} = 133.76 - 0.111T$, with $R^2 = 0.995$; benzene/water, $a_{bw} = 124.63 - 0.093T$; $R^2 = 0.987$. See text for details.

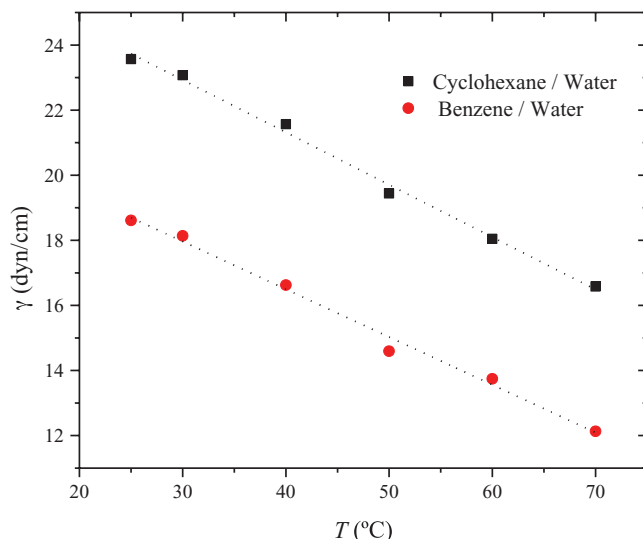


FIG. 4. Interfacial tension for cyclohexane/water (squares) and benzene/water (circles) mixtures at different temperatures T using DPD simulations with the repulsive interaction parameter taken from Table II, and shown also in Figure 3. The linear fits for the interfacial tension with T are: $\gamma = (27.76 \pm 0.3) - (0.1610 \pm 0.005)T$, with $R^2 = 0.994$ for cyclohexane/water, and $\gamma = (22.40 \pm 0.3) - (0.147 \pm 0.007)T$, with $R^2 = 0.989$ for benzene/water. See text for details.

state independent of the magnitude of the conservative force parameter.²² Values of the density higher than 3 raise the computing cost significantly. The constants in the dissipative and random forces were set to $\gamma = 4.5$ and $\sigma = 3$ in order to keep the temperature fixed at $k_B T = 1$. A reduced time step of $\Delta t^* = \Delta t(k_B T/mr_c^2)^{1/2} = 0.03$ was used during the simulation. The algorithm used for the numerical integration of the equation of motion is a version of the usual velocity-Verlet algorithm, adapted for the velocity-dependent dissipative force of the DPD model.³⁹ In each simulation 25 blocks with 10^4 time steps were performed and the properties of interest were calculated by averaging over the last 10 blocks. The total number of DPD atoms in all simulations was 4500 and the cubic box dimensions were $L_x^* = L_y^* = L_z^* = 11.4$. Periodic boundary conditions were imposed in all directions.

We studied systems constituted by a 50:50 mixture of DPD particles of water/benzene and water/cyclohexane at $T = 25, 30, 40, 50, 60$, and 70 °C. Three water molecules are represented in one DPD bead, corresponding to a coarse graining of $N_m = 3$. The benzene and cyclohexene molecules were each represented by one DPD bead. We used the parameters $a_{ij}(T)$ shown in Table II, for water/benzene and cyclohexane/water to perform DPD simulations at each of the temperatures listed above, keeping $a_{ii}(T)$ the same. The results for the interfacial tension between benzene/water and cyclohexane/water when T is varied are shown in Figure 4 for each system. As expected in all cases, the interfacial tension decreases when T is increased.

Using the correspondence between dimensional and adimensional interfacial tension, given by $\gamma_{calc} = (k_B T/r_c^2)\gamma_{DPD}$, one can compare directly with experimental data obtained by Albaz *et al.*⁴⁰ They obtain the interfacial tension for benzene/water and cyclohexane/water mixtures, among others, over a temperature range of 20–80 °C using an improved

TABLE III. Comparison between experimental data and the DPD simulations results obtained in this work.

System	Expt. ⁴⁰	DPD simulations (our work)
Benzene/water	$\gamma_{b/w}(\text{mN/m}) = 36.0$ $- 0.139T$ (°C)	$\gamma_{b/w}(\text{mN/m}) = (22.40 \pm 0.3)$ $- (0.147 \pm 0.007)T$ (°C)
Cyclohexane/water	$\gamma_{c/w}(\text{mN/m}) = 52.0$ $- 0.161T$ (°C)	$\gamma_{c/w}(\text{mN/m}) = (27.76 \pm 0.3)$ $- (0.161 \pm 0.005)T$ (°C)

methodology of the drop-weight method. A best-fit linear relationship between the interfacial tension and temperature was sought for each case, obtaining very good agreement between the slopes of our results and those of the experimental data reported. The results are summarized in Table III.

It is remarkable how well one can reproduce the experimental trends for the systems shown in Figure 4 and Table III using a coarse-graining procedure that, by its own structure, neglects atomistic details in favor of a mesoscopic view. It

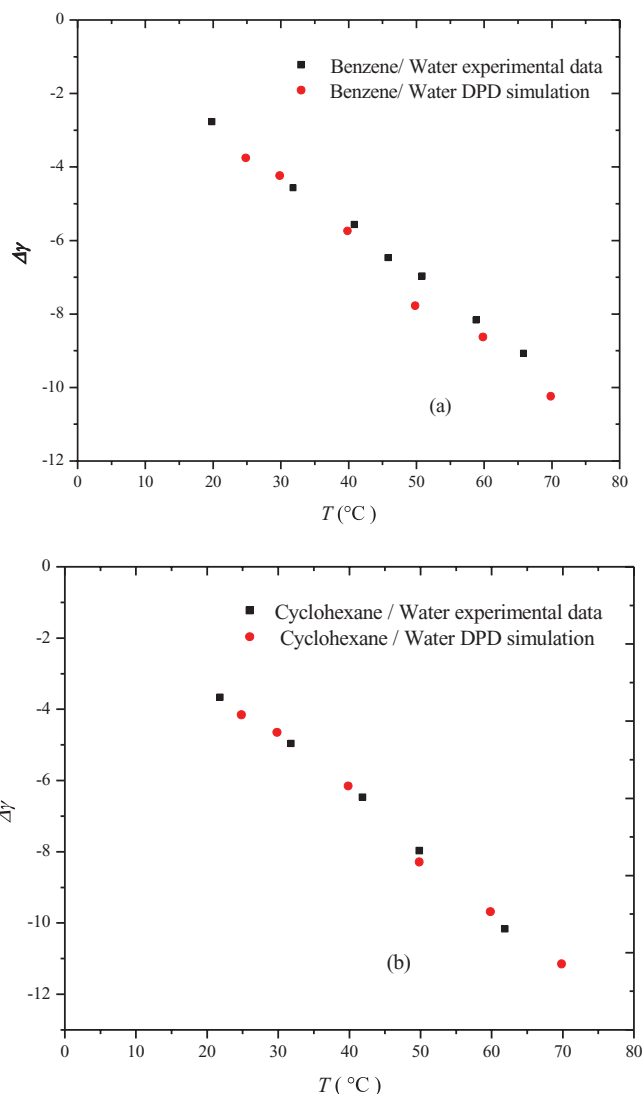


FIG. 5. Comparison of the experimental values for $\Delta\gamma = \gamma - \gamma_0$ (black squares) with the simulation results (red circles), as a function of temperature for (a) benzene/water; and (b) cyclohexane/water. The values for γ_0 were obtained from Table III in the limit when the temperature goes to zero.

is tempting to speculate that the temperature dependence of the a_{ij} parameters is responsible for the temperature dependence of the interfacial tension. However, one must be careful and recognize that if the temperature range is increased, and especially if long range electrostatic interactions are included, this may not be the case. Of course, one does expect for most systems that the interfacial temperature decreases as the temperature is raised and the interface becomes unstable, and it is clear this is the behavior our calculations predict (see Figure 4).

To stress how well our simulations reproduce the experimental trends, we show in Figure 5 the comparison of $\Delta\gamma = \gamma - \gamma_0$ as a function of temperature between our results and the available experimental data.⁴⁰ Although the $T = 0^\circ\text{C}$ value of the interfacial tension differs considerably between our predictions and the experimental results, this can be attributed to an artifact of the rescaling to physical units, see for example, Ref. 16 where it was shown that the actual value of the temperature-independent interfacial tension predicted

using different bead sizes was different. Those authors¹⁶ propose instead to use the experimental $\gamma(T = 0^\circ\text{C})$ to adjust the interaction parameters of the DPD model. However, our purpose is to show that the temperature dependence of the interfacial tension can be accurately predicted with DPD even if the temperature independent value is not obtained exactly. As one can see in Figure 5, the trends predicted by our simulations are in excellent agreement with the experimental ones.

The results presented in Figure 6 are the best fits of our data to a universal relation for the interfacial temperature as a function of temperature, $\gamma(T) = \gamma_0(1 - T/T_c)^\mu$, equivalent to the Guggenheim-Katayama-van der Waals model^{4,6} equation used for surface tension. Using the data and their linear fits, from Figure 4, we extrapolated the value of the interfacial tension (at $T = 0^\circ\text{C}$) and called it γ_0 . Extrapolating those fits to $\gamma(T) = 0$ we obtained the corresponding T_c value. Using this information, we show the reduced temperature dependence in Figure 6(a) for the benzene/water mixture, and in Figure 6(b) for the cyclohexane/water system, as well as their corresponding best linear fits (dotted lines). From the slope of those fits we get the value for the exponent μ , which is $\mu = 1.04 \pm 0.06$ for the benzene/water interface, and $\mu = 1.00 \pm 0.03$ for the cyclohexane/water interface. Hence, it can be taken as 1 for both systems, and it is smaller than the reported 11/9 value for the surface tension of organic liquids.⁴ Nevertheless, the fits shown in Figure 6 indicate that a generalized, reduced interfacial tension formula can be obtained for the systems we have studied, and that the exponent in such formula appears to be universal. Of course, more work is needed to validate this claim, but we believe the evidence in Figure 6 is encouraging.

V. CONCLUSIONS

The temperature dependence of the Flory-Huggins χ parameter suggests that the repulsive parameters a_{ij} in the conservative force component used in DPD simulations must also depend on T . A correct parametrization for these quantities is then obtained through the solubility coefficient at different T . DPD simulations aimed at obtaining the interfacial tension of an organic solvent and water were carried out, following the route of the temperature-dependent repulsive parameters previously calculated. Our simulations reproduce very well previously reported experimental results⁴⁰ for all the systems studied, displaying a decrease in the interfacial tension with increasing T .

The temperature dependence of the repulsive interaction DPD parameters obtained with our method (see Figure 3) appear to be qualitatively similar to that obtained by Travis *et al.*,¹⁸ so there may be more than one route to reach this goal. However, ours is a natural extension of the Groot and Warren method, and therefore should be easily accessible to researchers already familiar with the standard DPD model. Our predicted temperature dependence of the interfacial tension is, to the best of our knowledge, the first report for the DPD model. Additionally, we have found a scaling law for the temperature dependence of the reduced interfacial tension, with what appears to be a universal exponent $\mu = 1$. The reason why such scaling arises in our simulations is the robustness of the mean-field DPD approach, which is applied

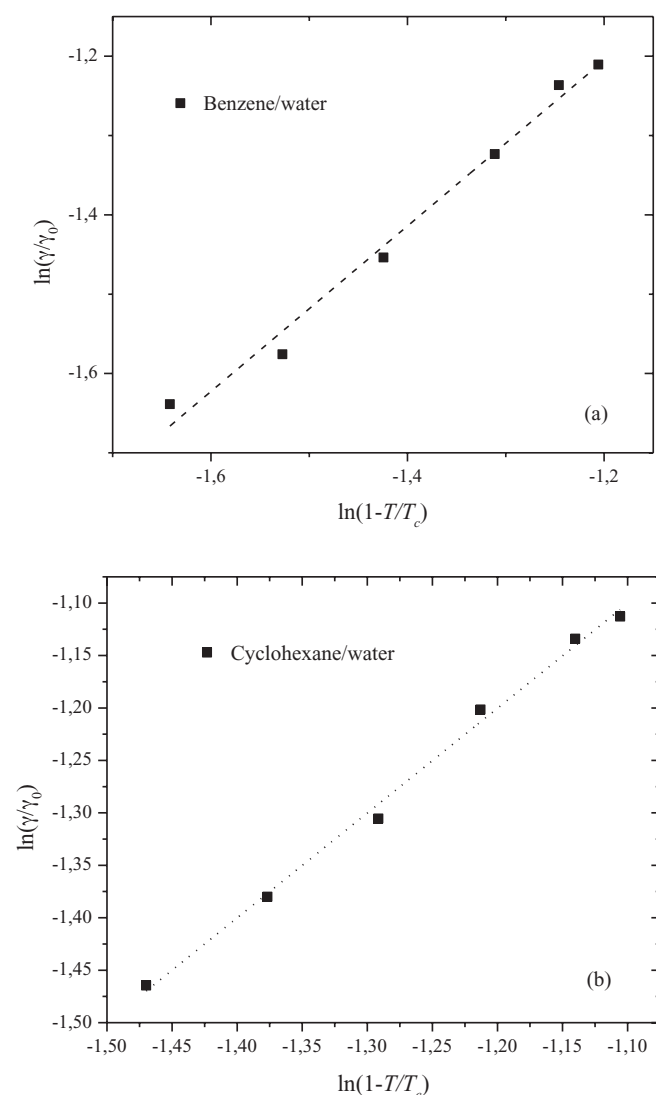


FIG. 6. $\ln(\gamma/\gamma_0)$ vs. $\ln(1 - T/T_c)$ to obtain the critical exponent μ from the equation $\gamma = \gamma_0(1 - T/T_c)^\mu$; the dotted lines are the best linear fits. (a) Benzene/water system with $\mu = 1.04 \pm 0.06$; and (b) cyclohexane/water with $\mu = 1.00 \pm 0.03$. See text for details.

for a system that, while not being near its critical point, does preserve the nearest neighbor interactions, which are responsible for the interfacial tension. That the universal exponent is 1 can be ascribed to the fact that the free energy of the interface, which is proportional to γ , can be expanded for temperatures near T_c , with the first (and dominant) term being exactly our prediction, $\gamma(T) = \gamma_0(1 - T/T_c)$, with higher order terms expected to contribute as the Hamiltonian of the system is improved. We believe these results are helpful for the understanding of the interfacial properties of fluids of current industrial and academic interest, and hope they will encourage further work on a more ample range of systems and temperatures.

ACKNOWLEDGMENTS

We are grateful to I. Soto Escalante for comments and discussions. A.G.G. wishes to thank K. Travis for enlightening discussions at the early phase of this project, and PROMEP, Project 47310286-912025; CONACyT's Project 105532 for support.

- ¹A. A. Rafati, E. Ghasemian, and M. Abdolmaleki, *J. Chem. Eng. Data* **53**, 1944 (2008).
- ²G. M. Ataev, *Russian J. Phys. Chem. A* **81**, 2094 (2007).
- ³S. H. Anastasiadis, I. Gancarz, and J. T. Koberstein, *Macromolecules* **21**, 2980 (1988).
- ⁴S. Wu, *J. Macromol. Sci., Polym. Rev.* **10**, 1 (1974).
- ⁵D. Villers and J. K. Platten, *J. Phys. Chem.* **92**, 4023 (1988).
- ⁶A. N. Kensington, *The Physics and Chemistry of Surfaces* (Oxford University, New York, 1941).
- ⁷E. Helfand and Y. Tagami, *J. Chem. Phys.* **56**, 3592 (1972).
- ⁸E. Helfand and A. M. Sapse, *J. Chem. Phys.* **62**, 1327 (1975).
- ⁹E. Helfand, *J. Chem. Phys.* **63**, 2192 (1975).
- ¹⁰M. P. Allen and D. J. Tildesley, *Computer Simulation of Liquids* (Oxford University, New York, 1987).
- ¹¹D. Frenkel and B. Smit, *Understanding Molecular Simulation* (Academic, New York, 2002).
- ¹²P. J. Hoogerbrugge and J. M. V. A. Koelman, *Europhys. Lett.* **19**, 155 (1992).
- ¹³L. Rekvig, M. Kranenburg, J. Vreede, B. Hafskjold, and B. Smit, *Langmuir* **19**, 8195 (2003).
- ¹⁴Y. Li, P. Zhang, F.-L. Dong, X.-L. Cao, X.-W. Song, and X.-H. Cui, *J. Colloid Interface Sci.* **290**, 275 (2005).
- ¹⁵A. Gama Goicochea, M. Romero-Bastida, and R. López-Redón, *Mol. Phys.* **105**, 2375 (2007).
- ¹⁶A. Maiti and S. McGrother, *J. Chem. Phys.* **120**, 1594 (2004).
- ¹⁷E. Mayoral and E. Nahmad-Achar, *J. Chem. Phys.* **137**, 194701 (2012).
- ¹⁸K. P. Travis, M. Bankhead, K. Good, and S. L. Owens, *J. Chem. Phys.* **127**, 014109 (2007).
- ¹⁹T. Murtola, A. Bunker, I. Vattulainen, M. Deserno, and M. Karttunen, *Phys. Chem. Chem. Phys.* **11**, 1869 (2009).
- ²⁰B. M. Forrest and U. W. Suter, *J. Chem. Phys.* **102**, 7256 (1995).
- ²¹P. Español and P. Warren, *Europhys. Lett.* **30**, 191 (1995).
- ²²R. D. Groot and P. B. Warren, *J. Chem. Phys.* **107**, 4423 (1997).
- ²³R. D. Groot, *J. Chem. Phys.* **118**, 11265 (2003).
- ²⁴J. H. Hildebrand and S. E. Wood, *J. Chem. Phys.* **1**, 817 (1933).
- ²⁵G. Scatchard, *Chem. Rev.* **8**, 321 (1931).
- ²⁶P. J. Flory, *J. Chem. Phys.* **10**, 51 (1942).
- ²⁷M. L. Huggins, *J. Chem. Phys.* **9**, 440 (1941).
- ²⁸M. G. Bawendi and K. F. Freed, *J. Chem. Phys.* **84**, 7036 (1986).
- ²⁹M. G. Bawendi, K. F. Freed, and U. Mohanty, *J. Chem. Phys.* **87**, 5534 (1987).
- ³⁰V. A. Baulin and A. Halperin, *Macromolecules* **35**, 6432 (2002).
- ³¹V. A. Baulin and A. Halperin, *Macromol. Theory Simul.* **12**, 549 (2003).
- ³²J. N. Owens, Ph.D. dissertation, Princeton University, Princeton, NJ, 1986.
- ³³F. M. Barton, *Chem. Rev.* **75**, 731 (1975).
- ³⁴R. F. Blanks and J. M. Prausnitz, *Ind. Eng. Chem. Fundam.* **3**, 1 (1964).
- ³⁵J. H. Hildebrand and R. L. Scott, *Regular Solutions* (Prentice-Hall, Englewood Cliffs, New York, 1962).
- ³⁶R. A. Fine and F. J. Millero, *J. Chem. Phys.* **59**, 5529 (1973).
- ³⁷See <http://www.accelrys.com> for more information on these and other suites.
- ³⁸H. Sun, *J. Phys. Chem. B* **102**, 7338 (1998).
- ³⁹I. Vattulainen, M. Karttunen, G. Besold, and J. M. Polson, *J. Chem. Phys.* **116**, 3967 (2002).
- ⁴⁰M. Albaz, A. Bilgesu, and O. Tutkun, *Commun. Fac. Sci. Univ. Ank. Serie B* **34**, 103 (1988).